Faraday Discuss. Chem. Soc., 1990, **89**, 000–000

Structure and Roughening of the Pt(110) Surface

Ian K. Robinson* and Elias Vlieg
AT&T Bell Laboratories, Murray Hill, NJ 07974, USA

Klaus Kern
IGV-KFA Jülich, D-5170 Jülich, Federal Republic of Germany

X-Ray diffraction using synchrotron radiation from the National Synchrotron Light Source at Brookhaven has been used to study the clean Pt(110) surface prepared in ultrahigh vacuum. Three-dimensional crystallographic data show the structure to be 'missing row' with alternate [0$\bar{1}$1] rows of atoms vacant in the top layer. Significant lateral relaxations are seen down to the fourth layer. Above 1080 K the surface undergoes a phase transition somewhat like that of Au(110). However, a distinct shifting of the half-order peak reveals the transition to involve the appearance of surface steps, and so it must be classified as a roughening transition instead of a simple 2D Ising model.

With the advent of second-generation synchrotron sources that are operated in a dedicated manner for the production of hard X-rays, there has been a rapid growth of interest in advanced diffraction experiments. The older machines, optimised for high-energy physics experiments, and often running on an infrequent schedule, made it hard to justify leaving complex and expensive equipment permanently stationed at a beamline. Portable experiments were designed instead so that the progress of whole research groups would not be held to ransom by operating schedules. We will describe a set of recent experiments carried out at the second-generation National Synchrotron Light Source (NSLS) in an end-station on beamline X16A that is customised for a single purpose: X-ray diffraction in ultrahigh vacuum (UHV).

The white beam is focussed by a toroidal mirror at 12.5 m onto the sample at 25 m. The resulting spot size is 1 mm × 1.5 mm. A double-crystal monochromator using Si(111) is 2 m before the sample and selects an energy in the range 5–13 kV. Normally the energy is changed only to avoid fluorescence from the sample or analyser crystal. The sample sits on the intersection of axes of a five-circle diffractometer inside the Be window section of a UHV chamber.[1] A pressure of 10^{-10} Torr† at the sample is maintained by turbo-, ion-, getter- and sublimation-pumps. Clean metal surfaces are prepared by ion bombardment and annealing, then characterised by Auger spectroscopy and low-energy electron diffraction (LEED).

The Pt crystal was cut and polished at Jülich to within 0.1° of the (110) crystallographic plane. Careful preparation was necessary to achieve a highly ordered surface. First it was heated extensively to 1200 K in 10^{-6} Torr O_2 to remove C impurities and sputtered with Ar^+ ions. Then it was annealed by gradually raising the temperature to 1000 K over an 8 h period; this resulted in the best ordered surface.

The diffraction measurements were made using the computer-controlled diffractometer. The diffraction geometry depended on the kind of measurement to be made. For high-temperature studies where the thermal diffuse background would be large, the grazing incidence geometry was used to minimise the penetration of the beam into the sample.[2] For three-dimensional crystallographic measurements, the five-circle mode[3]

† 1 Torr = 101 325/760 Pa.

was employed to gain out-of-plane momentum transfer. In both cases the exact angular direction of the surface normal was determined by optical reflection of laser light; this information was combined with the crystallographic orientation of two reference bulk Bragg reflections to determine the precise setting for each measurement.[2,3] In this way, no assumptions were needed about the exact cut direction of the surface. All diffraction settings referred to the reciprocal lattice of the crystal. Resolution was determined by the mirror aperture on the input and by 2 mm slits at 500 mm on the detector 2θ arm.

Structure Determination

The technique of surface X-ray crystallography has been reviewed recently.[4,5] Its basic distinction from bulk crystallography is due to the 2D nature of the diffraction itself. Instead of a lattice of sharp spots (3D δ-functions) we have an array of diffuse Bragg rods (2D δ-functions) in reciprocal space. The crystallographic information is contained in the profiles of these rods. A truly 2D structure would yield flat, featureless rod profiles. Most real surfaces contain structural modifications in more than one layer. This gives rise to modulations of the rods, which can be analysed by fitting to learn about the multilayer structure. This applies equally well to interfaces between two crystals or between a crystal and an amorphous or liquid region.[6]

It is important to isolate the diffraction from the surface or interface from that of the remainder of the sample, which has considerable more total scattering power. While grazing incidence helps to some extent here, this is best done by means of symmetry alone, particularly when accurate intensity data are needed. The bulk contribution is either three-dimensional or zero-dimensional (diffuse in all directions). We measure in places that are far away from the former, and subtract away the latter as background. This is particularly easy for a surface like Pt(110) that is reconstructed: its surface has lower translational symmetry than the bulk and gives rise to fractional-order superlattice reflections that are unambiguously distinguishable. The work reported here uses data only from such reflections.

Previous experimental work on the structure of Pt(110) has not been quite as extensive as work on Au(110), but clearly indicates a 'missing-row' structure for both surfaces. For most experimental groups, the symmetry is 1×2, implying that the reconstructed unit cell is doubled in the long direction of the rectangle parallel to [100]; one study[7] found in addition a way to make a stable 1×3 state (trebled unit cell) of the surface, but considered it might be stabilised by impurities. This uncertainty over the exact translational symmetry of Pt(110) is discussed further in the next section but here we will concentrate on the most studied 1×2 surface. The two LEED studies of Pt(110)[7,8] agree well with each other as well. The proposed model, shown in fig. 1, has the following features. Of the two atoms in the top layer of the unit cell, one is missing. The atom that remains is relaxed towards the bulk. The atoms in the second layer move out of the way by means of lateral displacements. Consequently, the third layer is buckled and the fourth has lateral displacements too. As fig. 1 shows, these are the displacements permitted by symmetry. The inward relaxation and the missing-row features are also confirmed by medium-energy ion scattering (MEIS).[9]

Theoretical work has also confirmed the missing-row structure for Pt(110) and Au(110).[10,11] An interesting aspect of this work is that the trends in the periodic table can be understood to some extent. Pt, Au and Ir(110) have stable missing-row structures. Unreconstructed Ag(110) is marginally stable but can adopt the missing-row structure when the Fermi level is perturbed by the deposition of a small amount of alkali metal.[12] Cu and Ni(110) are stable as unreconstructed surfaces.

X-Ray data were taken as scans of the diffractometer θ axis (rocking curves). This correctly accounts for both sample mosaic and disorder effects to give a true integration of the intensity, provided the peak is not broader than the 2θ resolution.[4] Integrated

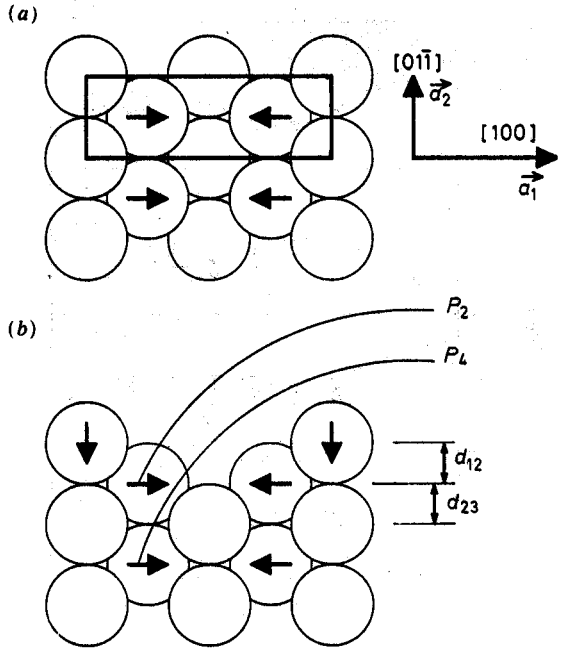

Fig. 1. Atomic model of the 1×2 missing-row structure. Arrows indicate symmetry-allowed displacements. Labels correspond to parameter values in table 1. (*a*) Top view, (*b*) side view.

intensity values were obtained as the area under the histogram minus background[4] then corrected for Lorentz factor (sin 2θ) and for the variation of active sample area[4] (sin 2θ). Structure factors (square root of intensity) were measured for eight half-order rods sampled at several values of perpendicular momentum transfer L to resolve the modulation of the continuous function $F_{hk}(L)$. We use the same indexing system as LEED, defining two in-plane reciprocal lattice vectors as $\boldsymbol{a}_1 = (100)_{\text{cubic}}$, $\boldsymbol{a}_2 = \frac{1}{2}(011)_{\text{cubic}}$ and the perpendicular reciprocal lattice vector $\boldsymbol{a}_3 = \frac{1}{2}(011)_{\text{cubic}}$. Examples of the rod data are given in fig. 2.

It is immediately clear from the rapid modulation of the rods that a multilayer structure is called for. The number of layer spacings involved can be estimated at *ca.* 3 which is the inverse period of modulation. These curves are extremely similar to those measured for Au(110)[13] and show a strong similarity between the structures, as expected. Moreover the corresponding parts of the (1.5, 0, L) and (2.5, 0, L) curves agree well with the much earlier rotating anode data for Au(110)[14]; these were interpreted in terms of a two-layer model with an enlarged spacing that is inconsistent with the new data. We find it necessary to include four layers with significant modification to obtain a good fit. The refined parameters,[13] quoted in table 1, are in good agreement with the most recent LEED papers[7,8] (see below) and consistent with the MEIS result, when it is considered that what is measured is effectively the alignment angle between the first and second layer atoms, thereby coupling in-plane and out-of-plane displacements.

Comparison with theory, table 1, is not quite so impressive. Both model calculations predict correctly that there is a contraction of the top-layer spacing, $\delta d_{12} < 0$, but only the embedded-atom calculation[11] attains the correct magnitude. The tight-binding calculation[10] grossly underestimates all the displacements, while the other has the second-layer pairing in the wrong direction. What is needed is a first-principles calculation with relaxation of four layers of coordinates.

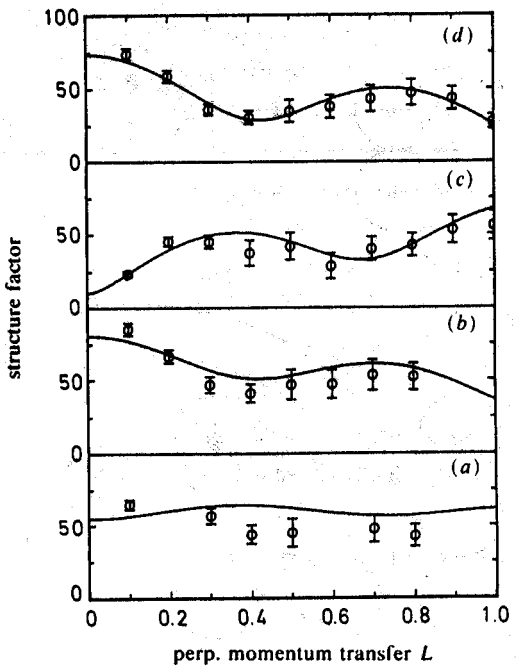

Fig. 2. Measurements of the structure factor $F_{hk}(L)$ along several reciprocal lattice rods for Pt(110). The line is the best fit to a missing-row structural model with parameters given in table 1.

We would like to reflect a little on the relative accuracy of determination of the various parameters with the aid of fig. 3. Pt(110) has suddenly become a well studied surface with state-of-the-art LEED and X-ray results to compare. It is also a relatively simple reconstructed surface with an agreed-upon structure and important structural parameters both parallel and perpendicular to the plane. It also displays simultaneously three contrasting modes of reconstruction: density modification (top layer), pairing (second and fourth layers) and buckling (third layer). Fig. 3 shows a side view of

Table 1. A summary of the structural results and the most relevant related work on Pt(110) $-(1\times2)$

	δd_{12}	δd_{23}	p_2	p_4	b_3
		experimental			
X-rays[a]	−0.27 (10)	−0.11 (8)	0.05 (1)	0.04 (1)	—
LEED[b]	−0.26 (3)	−0.18 (3)	0.07 (3)	0.12 (6)	0.32
LEED[c]	−0.28 (2)	−0.01 (2)	0.04	0.05 (4)	0.17
MEIS[d]	−0.22 (4)	0.06 (4)	<0.04	—	0.10
		theoretical			
tight-binding[e]	−0.11	0.02	0.02	—	—
embedded atom[f]	−0.25	−0.07	−0.03	0.04	0.11

[a] This work. [b] Ref. (8). [c] Ref. (7). [d] Ref. (9). [e] Ref. (10). [f] Ref. (11). All displacements are given in Å and the error in the last digit is indicated in parentheses. The definition of the parameters δd and p is explained in fig. 1. b_3 represents buckling in the third layer, with a positive value meaning an upward displacement of the third-layer atom without a first-layer atom above it.

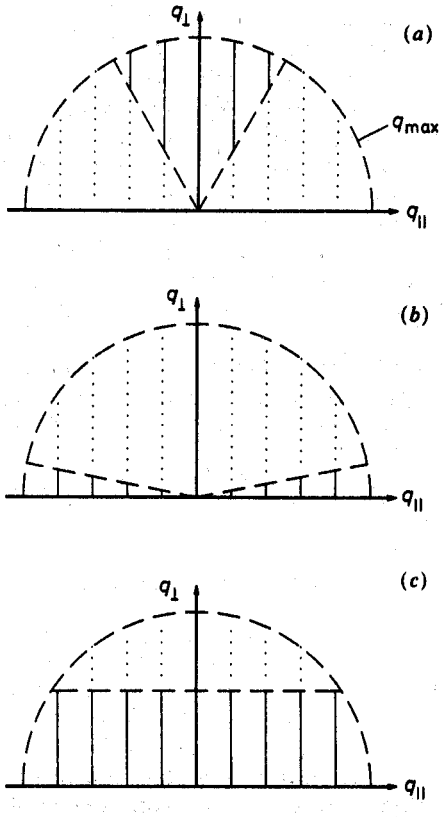

Fig. 3. Schematic reciprocal space diagrams showing the limited range of diffraction data available to different techniques. The rods represent data. The hemispherical diffraction limit is an arbitrary total resolution cut-off. (*a*) LEED: The cone angle is set by the angular size of the screen (120° here). LEED system designs might vary slightly but will not affect this picture dramatically. (*b*) Four-circle X-ray diffraction[2]: Here the cone angle is given by the maximum tilt angle accessible to the sample, limited by feedthroughs *etc.* (11° here[1]). The same tilting limitations and diagram apply to transmission electron diffraction (TED). (*c*) Five-circle X-ray diffraction[3] or X-ray diffraction with out-of-plane detector arm[5,17]: The limiting perpendicular limit is 'given by the wavevector times the maximum inclination angle (*ca.* 20°).

reciprocal space with rods representing the desired data in an ideal diffraction experiment (LEED or X-ray). A cut-off hemisphere is drawn to indicate some desired resolution limit: a complete, accurate set of measurements inside the sphere of radius q_{max} would allow the structure to be determined to an error of order 5% of $2\pi/q_{max}$ due to series termination effects[15] and depending somewhat on the accuracy of the data. This error would be isotropic. However, neither technique can measure the full hemisphere; a typical range of data is shown in the figure for LEED, four-circle[2] and five-circle[3] surface X-ray diffractometers.

LEED is primarily a back-scattering technique, probing mainly perpendicular momentum transfer. It is particularly sensitive to vertical displacements. It was able to detect third-layer buckling in Pt(110), that was beyond the level of significance of the X-ray data. Perpendicular distances are accurate in table 1; parallel ones are not. In the drawn-out history of the structure of the analogous Au(110), it was the discovery of the buckling, as well as the ability to handle such a large calculation, that led to the first really satisfactory agreement between LEED observation and calculation.[16]

Conversely, X-ray diffraction as most commonly practiced is a grazing-angle technique, with a correspondingly different subset [fig. 3(*b*)] of the data sampled. The four-circle (sample-tilting) geometry is particularly restrictive. So little was the range of data for the old Au(110)[14] study that it was unable to distinguish a top-layer expansion (albeit with an enormous error bar) in a two-layer model from a contraction in a four-layer model. The parallel displacement is also exaggerated by a factor of two, well outside the quoted error, for the same reason: two smaller displacements (second and fourth layers) were apparently indistinguishable from a single large one (second layer).

The extension to the five-circle mode has improved the situation significantly, as fig. 3(*c*) shows. The incident beam can be inclined to a large angle relative to the surface, improving the range of perpendicular momentum transfer. This is analogous to moving the detector out of plane[5,17]; the ability to do both is an anticipated further improvement. This was the geometry used in the present study. Parameters for Pt(110) in table 1 are still better determined in-plane than out of plane, but we have sufficient vertical information to avoid ambiguity in this and most other cases. More perpendicular resolution is needed to determine reliably the small (1–5%) layer spacing relaxations seen in many otherwise unreconstructed surfaces. LEED is still the best technique for this because of its great vertical sensitivity.

Thermal Roughening

We will use a slightly different definition of roughening from the conventional one that is discussed in theories of roughening: the divergence of the height-height correlation function. Instead we will refer directly to the distribution of surface steps. A surface with a high density of steps is rough, therefore roughness can be measured in a very direct way as step density. Rough surfaces can be made by sputtering and partial annealing, or may exist as the equilibrium state above the 'roughening temperature', T_R. Above T_R, the configurational entropy component of the free energy outweighs the energy cost of the steps.

Steps affect the diffraction from a missing-row reconstructed surface in a particularly dramatic way, provided the reconstruction extends right up to the steps on both sides. Because of the face-centring of the Pt lattice, each step acts as a domain wall with quadrature phase difference, which leads to shifted diffraction peaks. This was first seen on Au(110).[18] Since then it has been predicted that the shift should oscillate with perpendicular momentum transfer.[19] Now that we can make the required measurements, this is just what we find for Pt(110), as fig. 4 shows.

We can make a simple one-dimensional model to describe the shifted lineshape at the in-plane diffraction position, $L = 0$. We generalise the previous derivation[18] to include both the presence of quadrature steps (with total probability α) and conventional antiphase domain walls (with total probability β). Examples of some common surface defects as imaged by tunnelling microscopy[20] and their effective phase shifts are shown in fig. 5. These are also predicted to be the most stable line defect configurations theoretically.[21] As can be seen, both up and down single-height steps have the same phase shift of 1 (modulo 4) half-cell, while both kinds of antiphase defects have 2 (modulo 4). Step defects with a phase shift of three half-cells have also been postulated[22] but are rarely observed[20] and are energetically unfavourable.[21] The asymmetry with respect to defects of phase shift 1 (included) and 3 (omitted) half-cells is the essential aspect of the model that gives rise to shifted diffraction peaks. The new derivation[23] predicts a Lorentzian shape for the (1.5, 0, 0) peak with a half-width of $\beta/2+\alpha/4$ and a shift to higher momentum transfer of $\alpha/4$.

The temperature dependence of the lineshape was measured and found to behave reversibly. The data were fitted to adjustable Lorentzian lineshapes convoluted with the measured low-temperature lineshape; this latter function represents the known

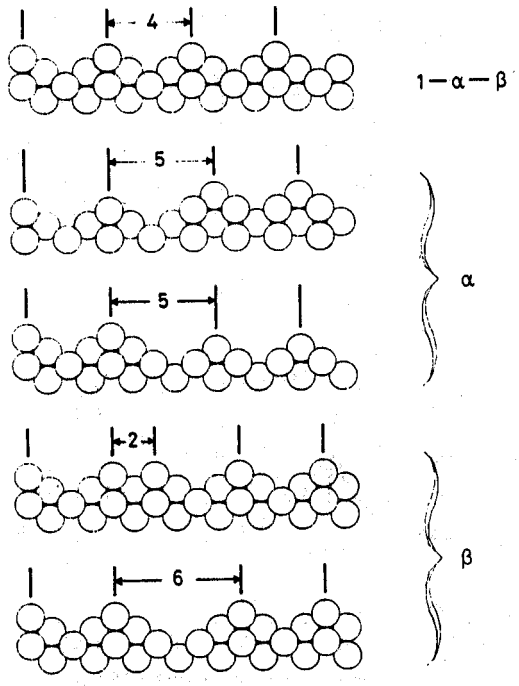

Fig. 4. Locus of the peak position in reciprocal space for a missing-row structure containing random steps, adapted from Fenter and Lu.[19] Superimposed on this are our data for Pt(110) on a normalised vertical scale, showing good agreement with the prior predictions.

instrumental resolution function as well as the residual finite size effects of the domain structure in the annealed sample. The dependence of the fitting parameters is shown in fig. 6. The height, $I(T)$, is explained by the theoretical curve, $I(T) = I_0|t|^{2\beta'}$ where $t = T/T_c - 1$ and $\beta' = 0.11 \pm 0.01$, and serves to identify the value of $T_c = 1080 \pm 1$ K (precision) ± 50 K (accuracy). The deviation from the ideal curve close to T_c is due to the appearance of critical scattering which was not modelled. Above T_c the half-width diverges linearly with t. Both of these aspects are exactly in accord with the 2D Ising model,[24] which has $\beta' = 1/8$ and $\upsilon = 1$ (correlation length exponent). Furthermore, they agree well with LEED data for the closely analogous phase transition for Au(110).[25] Strong symmetry arguments have been used to predict that missing-row structures should fall in the Ising universality class,[26] and Monte Carlo simulations have shown this to be in good agreement with the Au(110) results.[27]

Notwithstanding this apparent agreement between Pt(110), Au(110) and the 2D Ising model, we now turn to the last curve of fig. 6 showing peak shift *versus* temperature. This result is completely contrary to the Ising classification because it implies that steps form spontaneously above the phase transition. This immediately implicates some roughening character. Villain and Vilfan[22] had proposed that there might be separate roughening and Ising transitions close to the same temperature, but had not considered the possibility of a single transition with characteristics of both. If there are two transitions, they fall within 5 K of the same T_c, as fig. 6 shows. A six-vertex model has been used[28] more recently to describe the Au(110) surface theoretically; no Ising transition was found, but only a roughening transition instead. The lineshape model proposed in fig. 5 implies the missing-row ground state is now fourfold degenerate when steps are allowed, and so the correct universality classification could be a chiral four-state model.

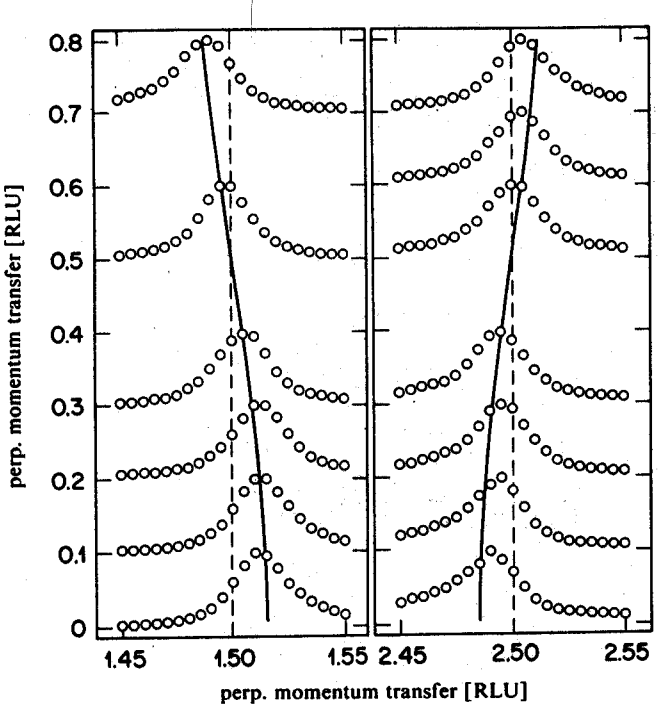

Fig. 5. Atomic models of Pt(110) surfaces containing a perfect (1×2) reconstruction (top), the same interrupted by a single height step (middle), and the same interrupted by antiphase defects (bottom). The lateral phase shift across the defect is indicated in units of half a unit cell spacing. α, β and $1-\alpha-\beta$ refer to the assumed probabilities per site of the various configurations.

The slopes of half-width *versus* T and peak shift *versus* T in fig. 6 allow us to quantify the relative probabilities of steps and antiphase defects using the expressions quoted above:[23] $\alpha = 6.6t$ and $\beta = 2.8t$. This means that thermally induced steps are 2-3 times more common than antiphase defects. The corresponding values for Au(110)[29] are $\alpha = 0$ and $\beta = 5.2t$, since no shift was seen. However, the spatial non-uniformities associated with LEED measurements in general make the technique rather insensitive to peak shifts. The published results[25,29] were made at an energy corresponding to $L = 0.5$ in fig. 4 where the shift should vanish: half the steps would be invisible and half would appear as antiphase domain walls. The quantity measured in the LEED experiment is therefore $\alpha/2+\beta$, which has a value $6.1t$ for Pt(110) and $5.2t$ for Au(110). The two surfaces are indeed similar, but the experimental question of whether steps are involved with the Au(110) 1×2 phase transition remains open.

The role of steps that appear spontaneously in Pt(110) as a function of temperature is a clear indication that the 1×2 reconstruction is only marginally stable. Theoretical studies showed that the free-energy difference between a 1×2 unit cell and step configuration is extremely small.[21] A 1×3 reconstruction comprising alternating up and down steps in a regular array is also a relatively favorable state, seen experimentally[7] and expected from theoretical work.[21,30] One way of understanding the shift of the diffraction peak is to consider that Pt(110) is tending, at elevated temperature, from a 1×2 state (peak at 1.5) to 1×3 (peak at 1.6667) by the random appearance of partial 1×3 unit cells, as in fig. 5. A recent X-ray diffraction study[31] of Au(110) actually found the 1×3 state to be more stable than the 1×2 state and that its phase transition shifted the peak in the opposite direction, from the 1×3 towards the 1×2. This suggests that the

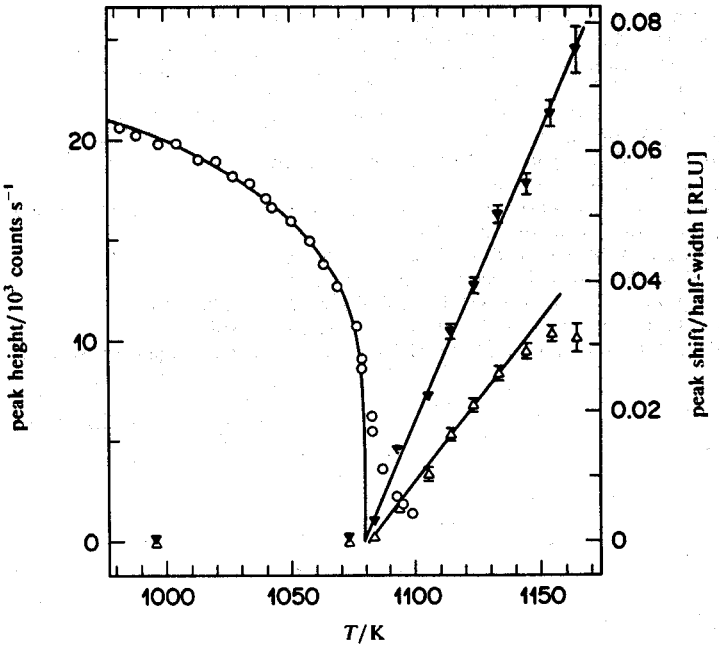

Fig. 6. Temperature dependence of the Lorentzian fitting parameters of the Pt(110) radial lineshape measured at (1.5, 0, 0.06). $T_c = 1080$ K, $\beta_c = 0.11$. ▼, Half-width; △, shift.

high-temperature state of this Au(110) crystal may be the same mixture of two- and three-atom wide facets as that seen on Pt(110) even though their low temperature structures have different translational symmetry.

We have enjoyed discussions of surface phase transitions with P. Bak, D. Huse, R. J. Birgeneau, T. L. Einstein and L. D. Roelofs. The crystal was expertly cut and polished by U. Linke at Jülich. NSLS is supported by the United States Department of Energy under contract DE-AC02-76CH00016.

References

1 P. H. Fuoss and I. K. Robinson, *Nucl. Inst. Meth.*, 1984, **222**, 171.
2 I. K. Robinson, *Rev. Sci. Instrum.*, 1989, **60**, 1541.
3 E. Vlieg, J. F. van der Veen, J. E. Macdonald and M. Miller, *J. Appl. Crystallogr.*, 1987, **20**, 330.
4 I. K. Robinson, in *Handbook on Synchrotron Radiation*, ed. D. E. Moncton and G. S. Brown (North-Holland, Amsterdam, 1989), vol. III, chap. 5, pp. xxx.
5 R. Feidenhans'l, *Surf. Sci. Rep.*, 1989, **10**, 105.
6 I. K. Robinson, W. K. Waskiewicz, R. T. Tung and J. Bohr, *Phys. Rev. Lett.*, 1986, **57**, 2714.
7 P. Fery, W. Moritz and D. Wolf, *Phys. Rev. B*, 1988, **38**, 7275.
8 E. C. Sowa, M. A. van Hove and D. L. Adams, *Surf. Sci.*, 1988, **199**, 174.
9 P. Fenter and T. Gustafsson, *Phys. Rev. B*, 1988, **38**, 10197.
10 H. J. Brocksch and K. H. Bennemann, *Surf. Sci.*, 1985, **161**, 321.
11 S. M. Foiles, *Surf. Sci.*, 1987, **191**, L779.
12 J. W. M. Frenken, R. L. Krans, J. F. van der Veen, E. Holub-Krappe and K. Horn, *Phys. Rev. Lett.*, 1987, **59**, 2307.
13 E. Vlieg, I. K. Robinson and K. Kern, *Surf. Sci.*, submitted.
14 I. K. Robinson, *Phys. Rev. Lett.*, 1983, **50**, 1145.
15 H. Lipson and W. Cochran, *The Determination of Crystal Structures* (Cornell University Press, 3rd edn, 1966), chap. 12, pp. 317-357.
16 W. Moritz and D. Wolf, *Surf. Sci.*, 1985, **163**, L655.

17 M. Nielsen, *Z. Phys. B*, 1985, **61**, 415.
18 I. K. Robinson, Y. Kuk and L. C. Feldman, *Phys. Rev. B*, 1984, **29**, 4762.
19 P. Fenter and T. M. Lu, *Surf. Sci.*, 1985, **154**, 15.
20 G. Binnig, H. Rohrer, C. Gerber and E. Weibel, *Surf. Sci.*, 1983, **131**, L379; T. Gritsch, D. Coulman, R. J. Behm and G. Ertl, *Phys. Rev. Lett.*, 1989, **63**, 1086.
21 L. D. Roelofs, S. M. Foiles, M. S. Daw and M. Baskes, to be published.
22 J. Villain and I. Vilfan, *Surf. Sci.*, 1988, **199**, 165.
23 I. K. Robinson, E. Vlieg and K. Kern, to be published.
24 L. Onsager, *Phys. Rev.*, 1944, **65**, 117.
25 J. C. Campuzano, M. S. Foster, G. Jennings, R. F. Willis and W. Unertl, *Phys. Rev. Lett.*, 1985, **54**, 2684.
26 P. Bak, *Solid State Commun.*, 1979, **32**, 581.
27 M. S. Daw and S. M. Foiles, *Phys. Rev. Lett.*, 1987, **59**, 2756.
28 A. C. Levi and M. Touzani, *Surf. Sci.*, 1989, **218**, 223.
29 J. C. Campuzano, G. Jennings and R. F. Willis, *Surf. Sci.*, 1985, **162**, 484.
30 M. Garofalo, E. Tosatti and F. Ercolessi, *Surf. Sci.*, 1987, **188**, 321.
31 G. A. Held, J. L. Jordan-Sweet, P. M. Horn, A. Mak and R. J. Birgeneau, *Solid State Commun.*, 1989, **72**, 37.

Paper 9/05299*B*; *Received 6th December*, 1989